

Poly(*para*-dioxanone) and Poly(*l*-lactic acid) Blends: Thermal, Mechanical, and Morphological Properties

A. P. T. Pezzin,¹ G. O. R. Alberda van Ekenstein,² C. A. C. Zavaglia,¹ G. ten Brinke,²
E. A. R. Duek¹

¹Universidade Estadual de Campinas, Faculdade de Engenharia Mecânica, Departamento de Engenharia de Materiais, Campinas, São Paulo, Brazil

²Laboratory of Polymer Chemistry and Materials Science Center, University of Groningen, Nijenborgh 4, 9747 AG Groningen, The Netherlands

Received 24 October 2001; accepted 8 September 2002

ABSTRACT: Blends of two semicrystalline polymers, poly(*l*-lactic acid) (PLLA) and poly-*p*-dioxanone (PPD) have been prepared by solvent casting in different compositions. Thermal, morphological, and mechanical properties of the blends were studied using modulated differential scanning calorimetry, wide-angle X-ray diffractometry, scanning electron microscopy (SEM), polarizing light microscopy (PLM), and tensile tests. Thermal analysis showed two glass transition temperatures nearly constant and equal to the values of the homopolymers and constant values of melting temperature (T_m) for all blend compositions, suggesting that both polymers are immiscible. The PLM and SEM observations validated these results, and showed the different morphology obtained by changing the composition of the blend. The

blends 40/60, 50/50, and 60/40 presented a clearly macroseparated system, while the 20/80 and 80/20 blends presented better homogeneity, probably due to the low amount of one component in the other. It was found by PLM that PPD is able to crystallize according to a spherulitic morphology when its content is above 40%. Under this content, the crystallization of PPD is hardly observed. The blend 20/80 is more flexible, and tough material and neck formation during elongation is also observed, due to PPD, which may act as a plasticizer. © 2003 Wiley Periodicals, Inc. *J Appl Polym Sci* 88: 2744–2755, 2003

Key words: biomaterials; bioreabsorbable polymers; blends; poly(lactic acid); poly(*p*-dioxanone)

INTRODUCTION

Aliphatic polyesters have been considered the most attractive family of polymers for biomedical applications. These polymers are of potential interest because they are bioreabsorbable and biocompatible. Nowadays, the most important members of this family are the poly(α -hydroxy acids) such as poly(lactic acid) (PLA), poly(glycolic acid) (PGA), poly(ϵ -caprolactone) (PCL), poly(β -hydroxybutyrate) (PHB), and poly-*p*-dioxanone (PPD).¹ Their degradation mechanisms have been attributed to a simple hydrolytic process. Ester bonds react with water, and are broken down to form carboxy and hydroxy terminal groups.² The lactic acid that is generated when PLA degrades is incorporated into the Krebs cycle and excreted by the lungs as carbon dioxide and water.³ PLA has three stereoisomers: poly(*l*-lactic acid) (PLLA), poly(*d*-lactic acid) (PDLA), and poly(*d*, *l*-lactic acid) (PDLLA). PLLA and PDLA are mirror images of one another in their structure, both

being optically pure, and crystalline,^{4,5} while PDLLA is racemic and amorphous.⁶ PLLA is a polyester with a melting temperature (T_m) around 180°C and glass transition temperature (T_g) of 65°C.⁷ Due to its high crystallinity, PLLA has poor mechanical properties, crazes easily, and shows slow degradation rate, limiting its medical applications.^{7,8} On the other hand, PPD is a highly flexible polymer with good tensile strength^{9–11} and rapid degradation rate.^{12,13} As a result of blending PLLA with PPD, it is expected that the degradation rate of PLLA will be accelerated and the mechanical properties further improved. In the past several years, the bioreabsorbable polymers are also have gained increasing importance in the medical field.¹⁴ Naturally the search for new improved bioabsorbable polymers has piqued a growing interest. Polymer blends have shown to be an excellent way for developing new materials, often exhibiting combinations of properties superior to either of the pure components.^{15,16} They represent a more cost-effective way of modifying properties than its chemical modification.¹⁷ Some characteristics such as mechanical properties and degradation behaviour can be modified by a favorable choice of the second component of the blend. Thus, the final properties will depend not

Correspondence to: E. A. R. Duek (eliduek@fem.unicamp.br).

TABLE I

PLLA/PDLA	Ikada (1987), ²⁰ Tsuji (1991, ²¹ 1991, ²² 1991, ⁵ 1992, ²³ 1992, ²⁴ 1993, ²⁵ 1994, ²⁶ 1999 ²⁷)
PLLA-co-PDLA/PLLA-co-PDLA	Tsuji (1992) ²⁸
PLLA/PDLA	Tsuji (1995, ²⁹ 1996, ³⁰ 1997. ⁶)
PLLA/PLLA-co-PCL	Cha (1990) ³¹
PLLA/PLLA-co-PGA	Cha (1990) ³¹
PLLA/PLLA-co-PCL	Dijkstra (1991) ³²
PLLA/PHB	Blümm (1995) ³³
PLLA/PFB-co-HV	Iannance (1994), ¹⁷ Ferreira (2001) ³⁴
PLLA-co-PGA/PDLA-co-PGA	Tsuji (1994) ²⁶
PHB-co-HV/PCL	Dave (1990) ³⁵
PDLA/PHB-co-HV	Dave (1990) ³⁶
PDLLA/PCL	Zhang (1995), ³⁷ Tsuji (1996), ³⁸ Domb (1993) ³⁹
PDLLA/PDLA	Tsuji (1997) ⁶
PDLLA/PHB	Zhang (1995, ³⁷ 1996 ⁴⁰)
PHB/PHB-co-HV	Organ (1994) ⁴¹
PHB/PCL	Zhang (1995), ³⁷ Gassner (1994), ⁴² Yasin (1993), ⁴³ Kumagai (1992) ⁴⁴

only on the chemical composition of the blend but also on its physical characteristics, such as glass transition temperature, crystallinity, and morphology, which are a direct consequence of the miscibility between the components in the blend. Blends in which both components are semicrystalline polymers have received less attention than fully amorphous or amorphous/semicrystalline systems. Semicrystalline/semicrystalline polymer blends, however, may provide new insights into the miscibility, crystallization behavior, and morphology of polymer blends in general.¹⁸ With respect to polymer blends with bioabsorbable components we can distinguish two main types: blends composed of a degradable polymer and a nondegradable polymer and blends composed of degradable polymers.¹⁹ Table I displays the bioabsorbable blend pairs that have been investigated.

The mixture of the polymers can be used to obtain materials with new degradation characteristics,³¹ and physical³⁰ and mechanical properties.⁴⁰ The bibliographic review showed that the study of bioabsorbable blends has not been much explored. The blend PPD/PLLA and about PPD with other polymers was not found in the literature. Most of the work has been mainly devoted to the study of the miscibility of PLLA, PDLA, and PHB with other polymers and copolymers. The method of preparation, the composition, and the molecular weight of the components seems to influence the final properties, degradation rate, and miscibility of the blends. However, miscibility is not always required when a bioabsorbable polymer is mixed with another.³³ In the present work we have investigated the miscibility of PPD/PLLA blends prepared by solvent casting. The miscibility of the blends was determined by measuring their glass transition temperature (T_g) using modulated differential scanning calorimetry (MDSC). Polarizing light microscopy

(PLM) and scanning electron microscopy (SEM) were used to study the crystallinity and phase morphology of the blends. Wide-angle X-ray diffractometry (WAXS) and tensile tests were used, respectively, to characterize the crystalline structure and to investigate the mechanical properties of the blends. The aims were to understand the basic physical phenomena involved on blending these two polymers, and to attempt to obtain a material with optimized properties to be used in the medical field. The virtual certainty that these blends are fully bioabsorbable served as further motivation for this work.

EXPERIMENTAL

Materials

PLLA used in this study was supplied by PURAC (Groningen, The Netherlands) with $M_w = 100,000$ daltons. PPD was obtained from Johnson & Johnson (São Paulo, Brazil) in the form of violet polydioxanone

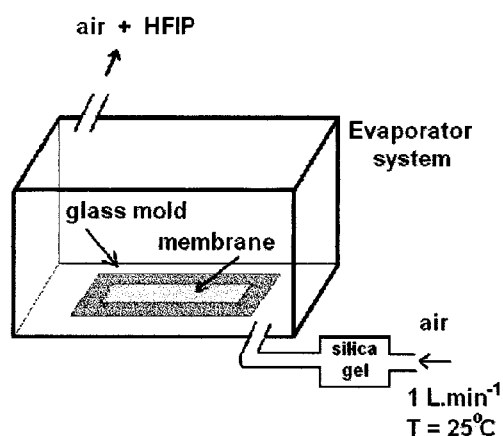


Figure 1 Evaporator system to obtain membranes by solvent casting.⁴⁵

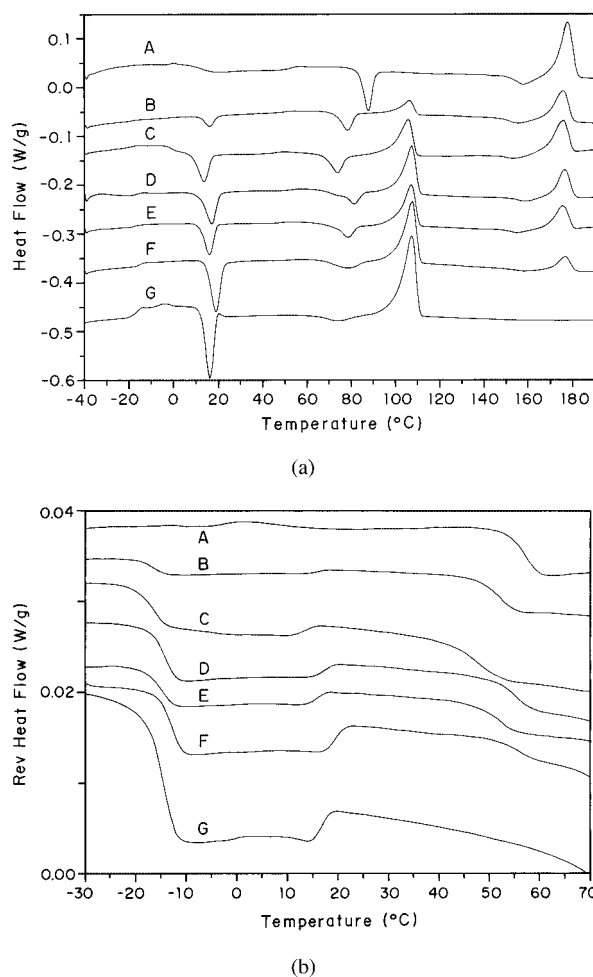


Figure 2 Curves obtained by MDSC for PPD/PLLA blends after quenching: (a) Total heat flow and (b) reversing heat flow. (A) 0/100, (B) 20/80, (C) 40/60, (D) 50/50, (E) 60/40, (F) 80/20, (G) 100/0.

sutures (PDS®). The dye was completely extracted in methylene chloride (Synth, São Paulo, Brazil) with magnetic mixing for 24 h at room temperature prior to use. Hexafluoroisopropanol (HFIP) was purchased from Aldrich (Milwaukee, WI).

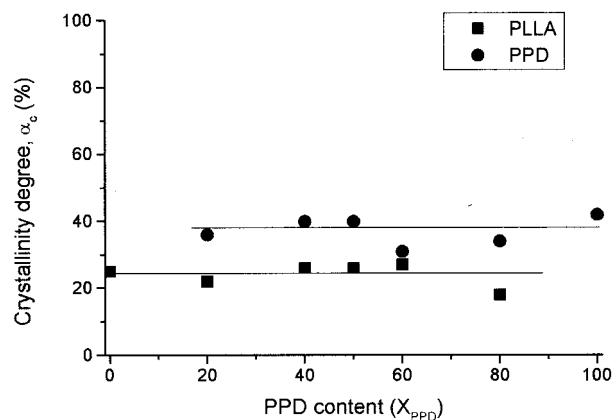


Figure 3 Crystallinity degree of PLLA (χ_c PLLA) and PPD (χ_c PPD) for all blends compositions, obtained from MDSC data for the PPD/PLLA blends.

Blend preparations

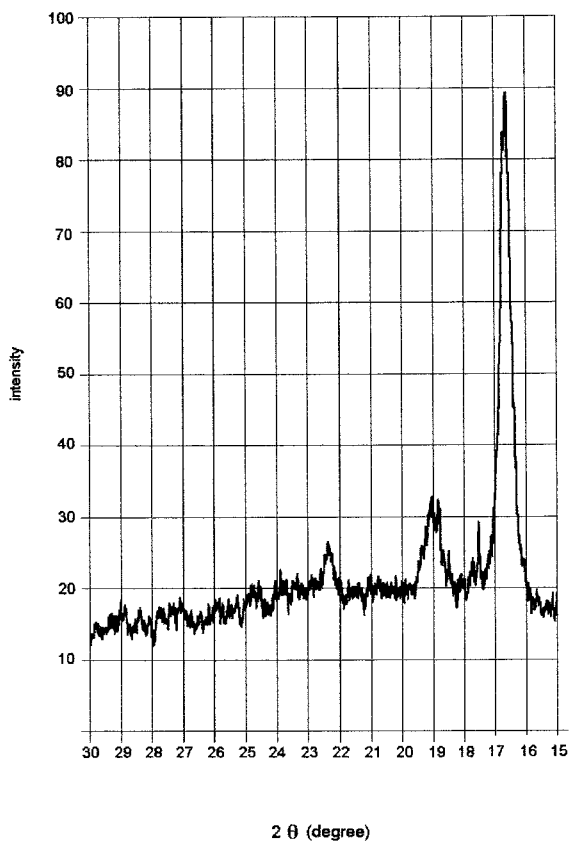
Films of PPD/PLLA blends with weight ratios of 0/100, 20/80, 40/60, 50/50, 60/40, 80/20, and 100/0, were prepared by solvent casting at room temperature. PLLA and PPD were dissolved separately in HFIP to form 10 w/v % solutions. The solutions with the different compositions were made by mixing of the appropriate amounts of the separate solutions and after magnetic mixing for 2 h until completely homogenized at room temperature. The mixture was poured in a glass mold (50 × 30 × 5 mm) and placed in an evaporator system for 24 h (Fig. 1). The films were dried in a vacuum oven at 60°C for 24 h and stored in a desiccator.

Modulated differential scanning calorimetry

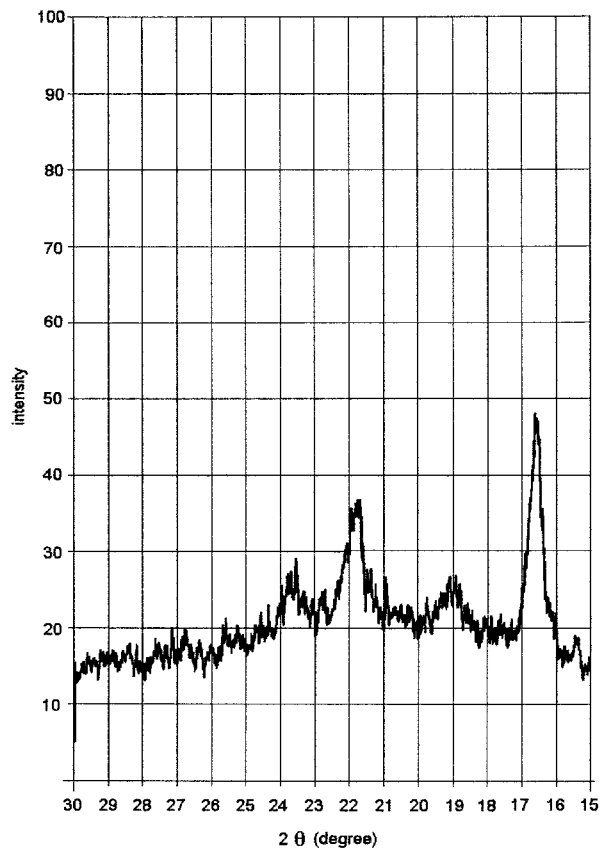
MDSC measurements were performed with a MDSC 2920 of TA instruments. Samples of 3–5 mg sealed in aluminum pans were annealed for 1 min at 200°C. Subsequently, they were quenched in liquid nitrogen and put in the MDSC at −40°C. The measurements were taken in a temperature interval from −40 to

TABLE II
Thermal Properties of the PPD/PLLA Blends

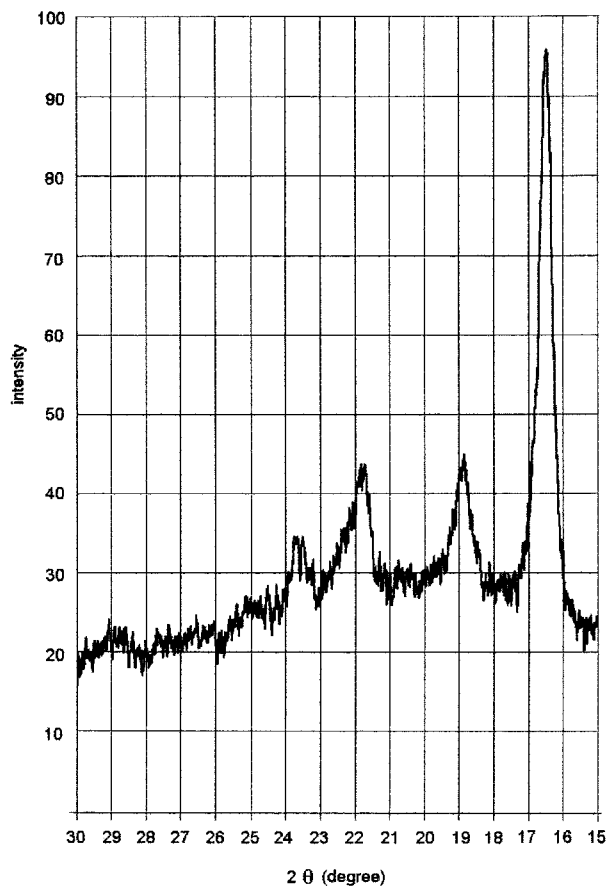
PPD/PLLA blends	T_g	T_c	ΔH_c	T_m	ΔH_m	T_c	T_c	ΔH_c	T_m	ΔH_m
	PPD (°C)	PPD (°C)	PPD (J g ⁻¹)	PPD (°C)	PPD (J g ⁻¹)	PLLA (°C)	PLLA (°C)	PLLA (J g ⁻¹)	PLLA (°C)	PLLA (J g ⁻¹)
0/100	–	–	–	–	–	57	88	26	178	49
20/80	–16	16	34	106	71	52	79	17	176	38
40/60	–16	14	48	106	89	48	74	30	176	54
50/50	–14	17	46	107	87	55	82	27	176	51
60/40	–15	16	32	107	64	52	79	31	175	56
80/20	–13	19	40	108	75	56	79	37	177	54
100/0	–14	16	36	108	79	–	–	–	–	–



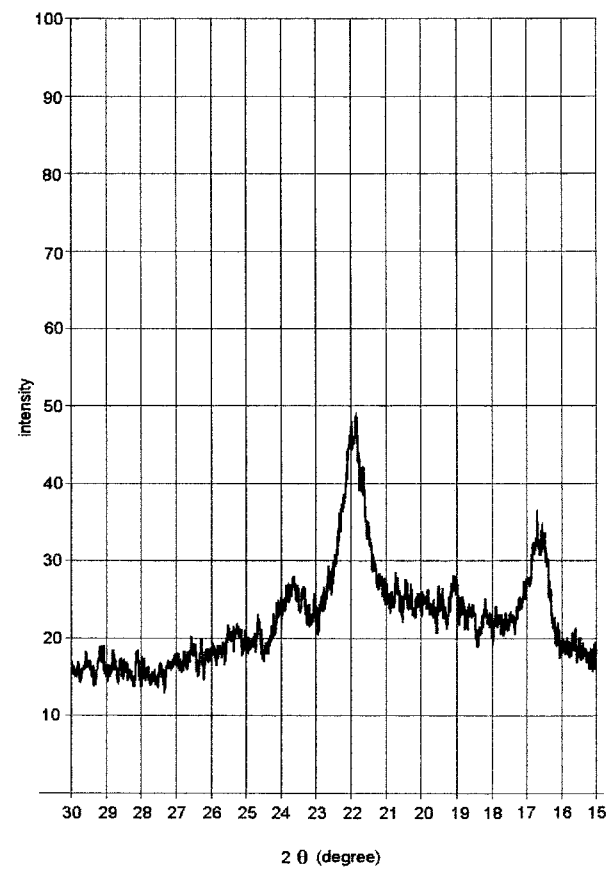
(a)



(c)



(b)



(d)

Figure 4 X-ray diffractions of the PPD/PLLA blends. (a) 0/100, (b) 20/80, (c) 40/60, (d) 50/50, (e) 60/40, (f) 80/20, and (g) 100/0.

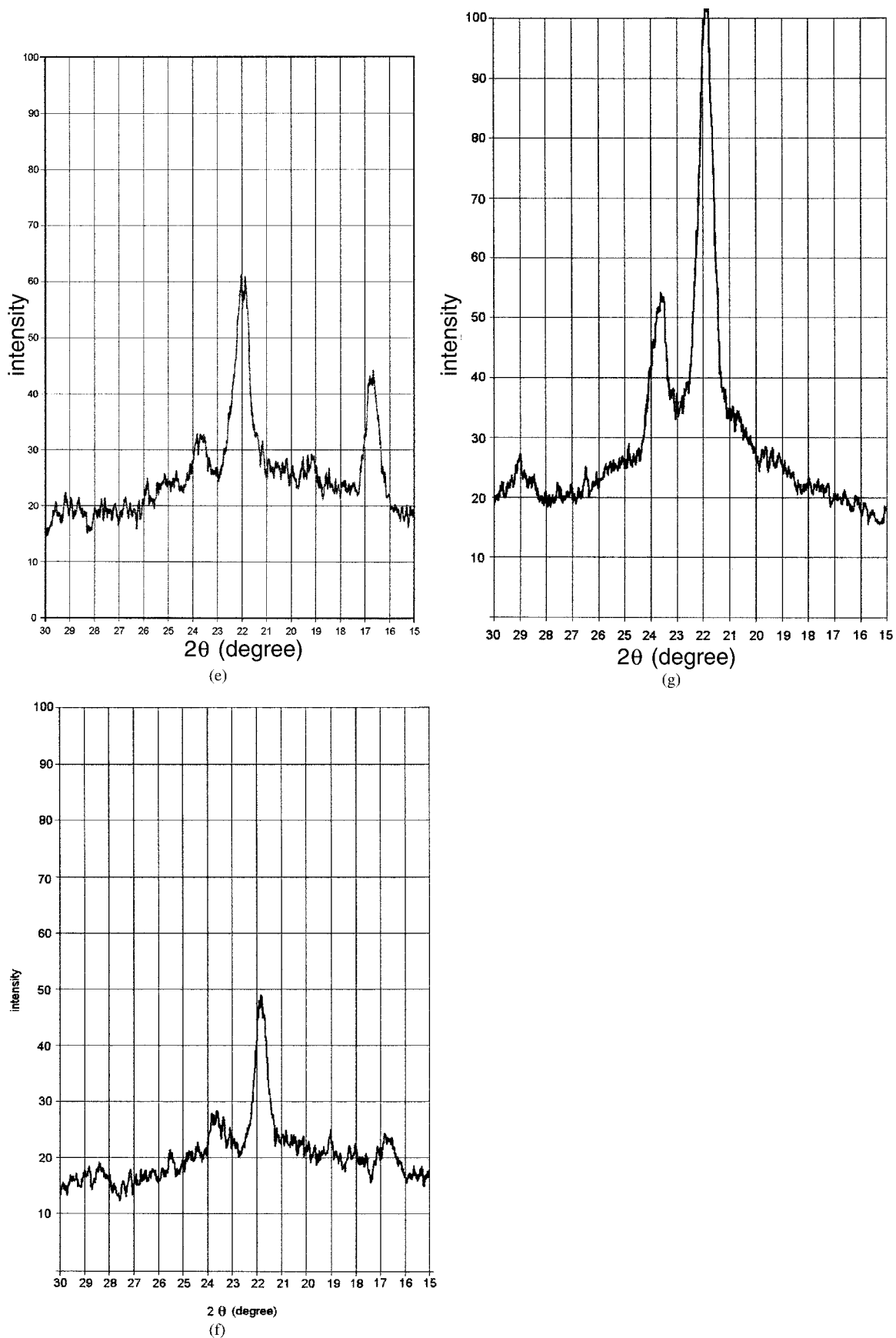


Figure 4 (Continued from the previous page)

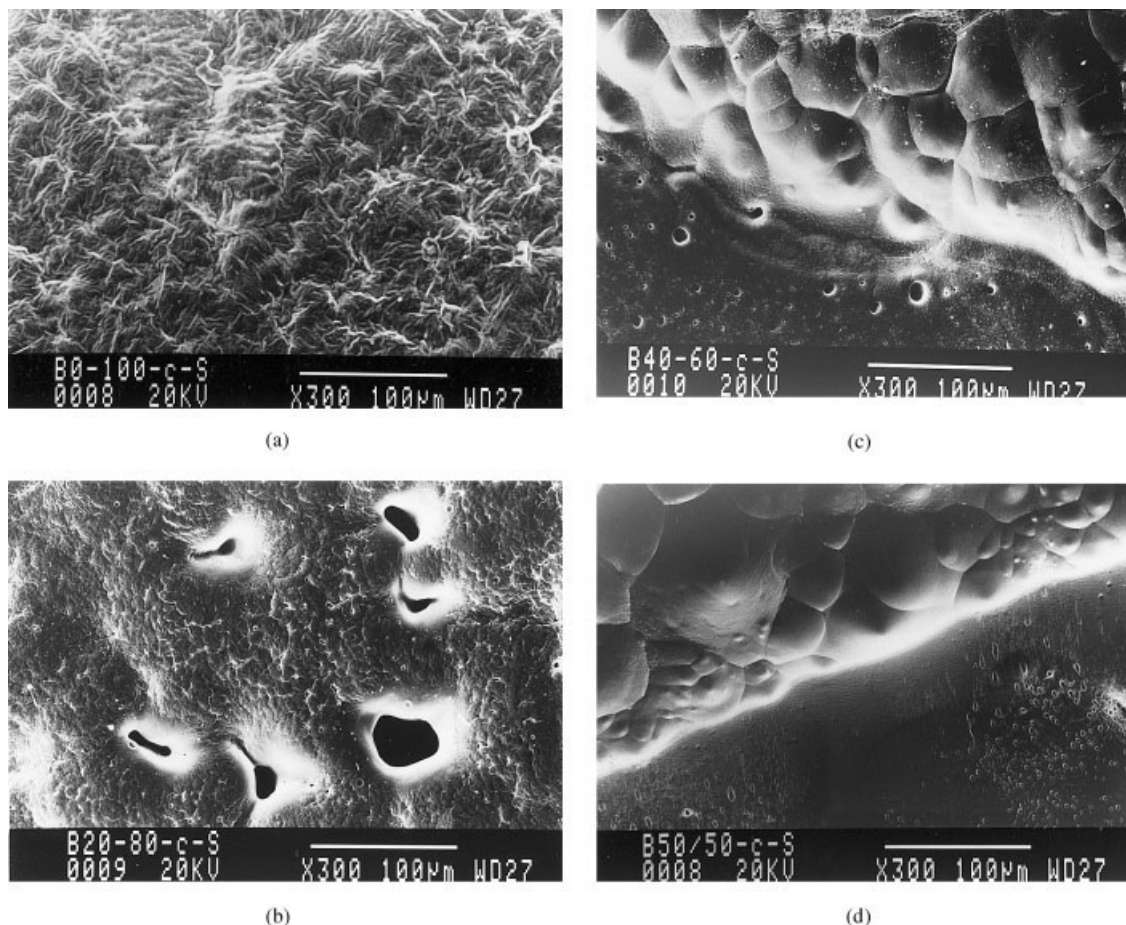


Figure 5 SEMs of surface of the PPD/PLLA blends. (a) 0/100, (b) 20/80, (c) 40/60, (d) 50/50, (e) 60/40, (f) 80/20, and (g) 100/0.

190°C. The underlying heating rate was $1^{\circ}\text{C min}^{-1}$. An oscillation amplitude of 0.5°C and an oscillation period of 60 s were used. The glass transition temperatures (T_g 's) were determined from the reversing heat flow curve.⁴⁶ The miscibility of the blends was investigated according to glass transition temperature.

Wide-angle diffraction

WAXDs were obtained in transmission using a Rigaku Geigerflex powder diffractometer. The radiation used was $\text{CuK}\alpha$ in the angular range 15° – 30° .

Polarizing light microscopy

Films of about $40\ \mu\text{m}$ thickness pressed in cover glasses were obtained by melt pressing at 200°C for 1 min using $34\ \text{kg cm}^{-2}$. Before crystallization, samples sandwiched between object glass and cover glass were first heated up to 200°C for 1 min in a Mettler FP82 hot stage, after which they were cooled with a very low cooling rate to the desired temperature of crystallization, $T_c = 65^{\circ}\text{C}$ for the PPD and $T_c = 130^{\circ}\text{C}$ for the

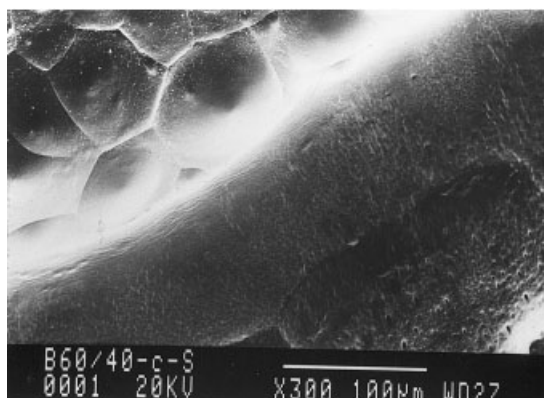
PLLA. A Zeiss Axiophot polarizing microscope equipped with a hot stage was used to visualize the morphology. The resulting morphologies were studied as a function of blend composition.

Scanning electron microscopy

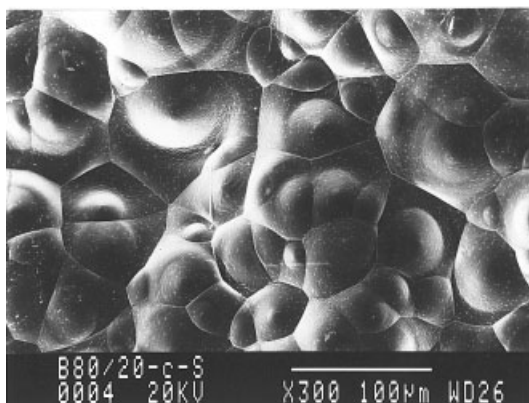
SEM evaluation was carried out to examine the phase morphology of the blends. A scanning electron microscopy (JEOL- JXA 840A) was used to observe the upper surfaces and samples fractured in liquid nitrogen, which were coated with a thin layer of gold by vacuum deposition, using a Sputter Coater BAL-TEC SCD 050.

Mechanical properties

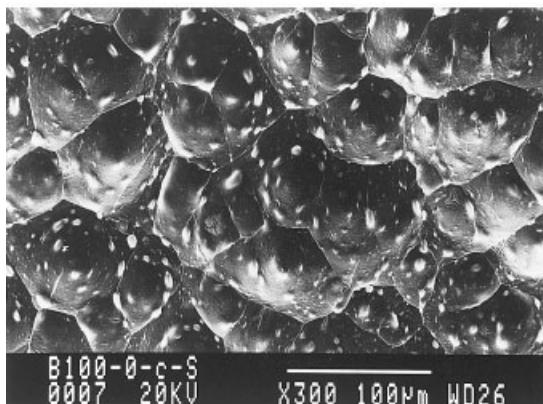
Tensile properties of the films ($40 \times 2 \times 0.2\ \text{mm}$) were studied by an Instron, Series IX Automated Materials Testing System 1.09 at 22°C and 50% relative humidity using a crosshead speed of $10\ \text{mm min}^{-1}$ and 100 N detector cell according to American Society for Testing and Materials standard



(c)



(f)



(g)

Figure 5 (Continued from the previous page)

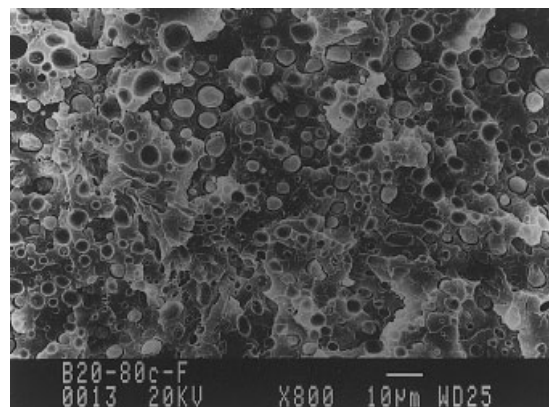
ASTM D882-75. The results were averaged from 5 tests per sample.

RESULTS AND DISCUSSION

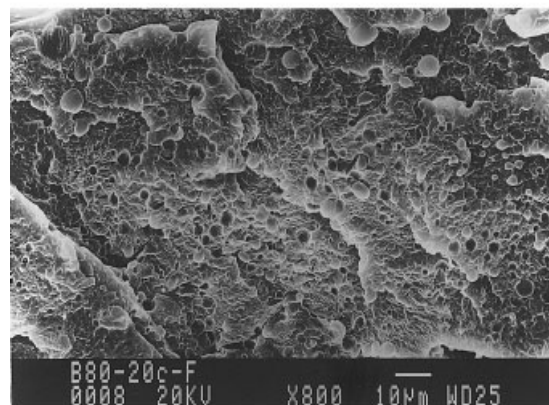
Modulated differential scanning calorimetry

Curves obtained by MDSC from the melt for the different pairs of blends and for the homopolymers, after

quenching, are shown in Figures 2(a) and 2(b). The glass transition temperature (T_g), crystallization peak temperature (T_c), crystallization enthalpy (ΔH_c), melting peak temperature (T_m), and melting enthalpy (ΔH_m) of PPD/PLLA blends were determined from MDSC thermograms. The results are summarized in Table II. The quenching treatment was done to better visualize the glass transitions by increasing the amorphous part in the sample. MDSC curves showed T_g s at -14 and 57°C for the PPD and PLLA, respectively. Two distinct and nearly constant T_g s and equal to the values of the homopolymers can be observed for all blend compositions, suggesting immiscibility of the system. Two endothermic peaks, due to the melting of PPD and PLLA, can be observed at 108 and 178°C , respectively. The constant values of T_m observed for the system PPD/PLLA in function of composition are also indication of immiscibility [Fig. 2(a)]. Studies of PHB/PCL, PHB-HV/PLLA, and PHB/PDLA blends also presented two distinct T_g s and constant values of T_m for all compositions, indicating the immiscibility of the



(a)



(b)

Figure 6 SEMs of fracture surface of the blends PPD/PPLA. (a) 20/80 and (b) 80/20.

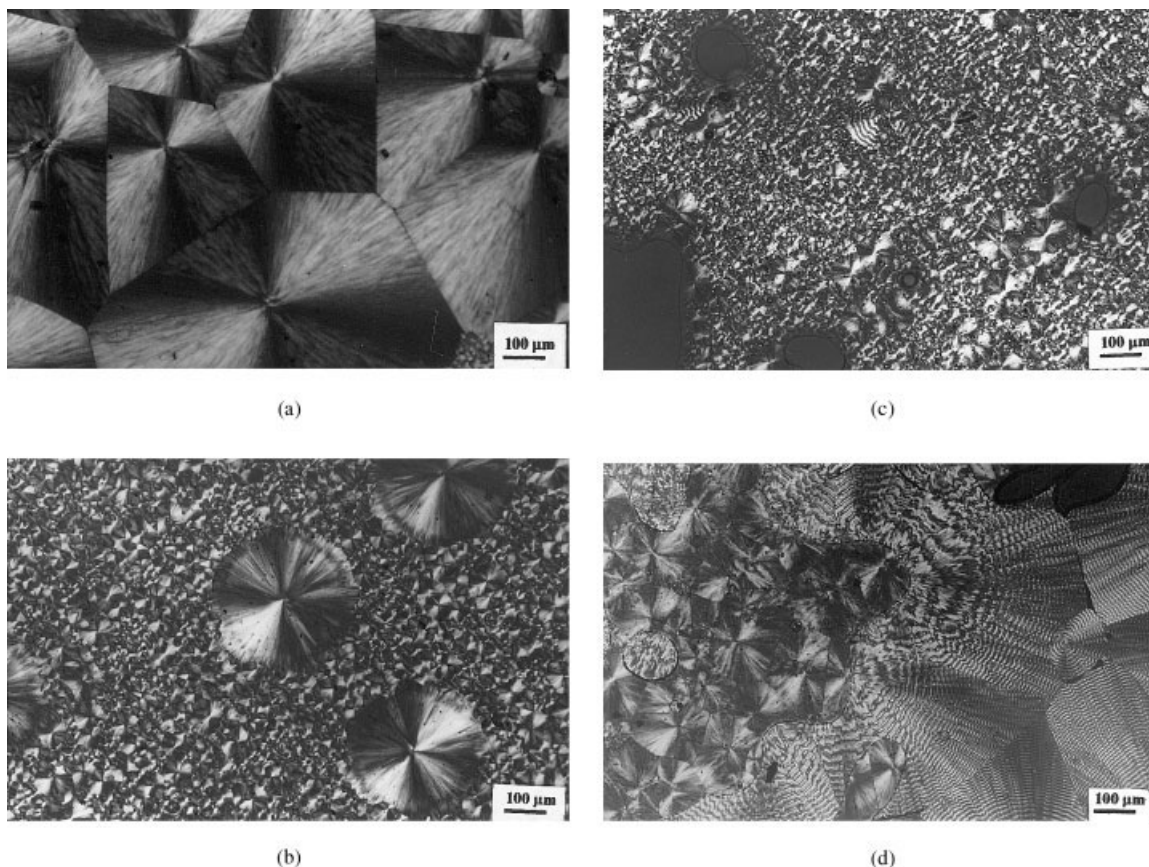


Figure 7 Cross-polarized optical micrographs describing the spherulitic structure of the PPD/PLLA blends grown at 65 and 130°C. (a) 0/100, (b) 20/80, (c) 40/60, (d) 50/50, (e) 60/40, (f) 80/20, and (g) 100/0.

system.^{36,38,40} The T_c of PPD is constant for all blend compositions, but we can observe that the position of T_c of pure PLLA is composition dependent (Table II). The T_c of pure PLLA is higher than the T_c of PLLA in the blends. This result indicates that the PPD component shows a remarkable effect on the crystallization of PLLA in the blends. This result may be explained by the fact that when PLLA crystallizes there are already PPD crystallites present, which may interfere, resulting in a crystallization at lower temperature, which gives a decrease of the T_c for PLLA and the amount of PPD does not influence this T_c . A similar result was also observed for poly(β -hydroxybutyrate)/poly(DL-lactide) blends.⁴⁰ The area related to the melting peak is associated with the enthalpy of melting (ΔH_m) of the crystalline phase. The ΔH_m values of PPD and PLLA were normalized with reference to their respective concentration. The ΔH_m values of both polymers in the blends were constant within experimental errors. From data of ΔH_m , ΔH_c , and calculated melting enthalpy considering the polymer 100% crystalline, $\Delta H_m^\circ = 93.7 \text{ J g}^{-1}$ for the PLLA⁴⁷ and $\Delta H_m^\circ = 102.9 \text{ J g}^{-1}$ for the PPD,⁴⁸ it was possible to obtain the

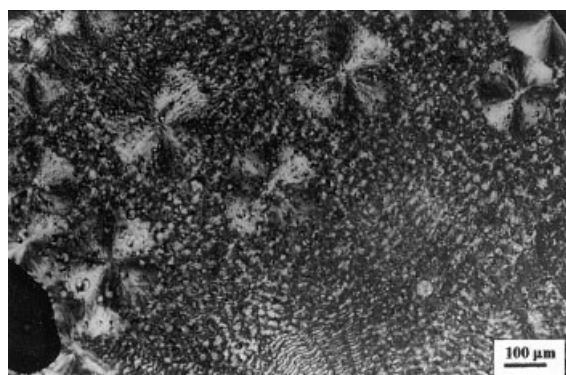
crystallinity degree (χ_c %) of PLLA and PPD in the blend, following

$$\chi_c = \frac{\Delta H_m - \Delta H_c}{\Delta H_m^\circ} \times 100 \quad (1)$$

Figure 3 shows that the crystallinity degree of PLLA (χ_c PLLA) and PPD (χ_c PPD) are constant for all blends compositions.

Wide-angle diffraction

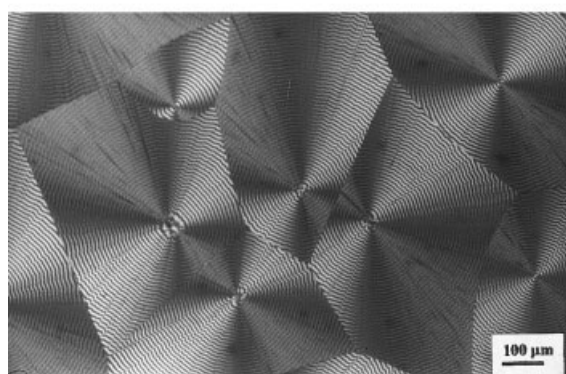
The diffraction profile for the homopolymers and the blends is shown in Figure 4. As can be seen, the diffraction peaks appear at 2θ around 16.5°, 19°, and 22.5° for the PLLA, whereas the PPD has the diffraction peaks appearing at 2θ equal to 22°, 23.5°, and 29°. The intensity of the diffraction peaks of PLLA decreases as PPD is added to the blends. The diffraction peaks of the blends involve all the peaks corresponding to the homopolymers. The diffraction profile for PLLA is identical with the pattern shown by Ikada,



(c)



(f)



(g)

Figure 7 (Continued from the previous page)

which are comparable with the results for the crystalline phase α of PLLA, which has a pseudo-orthorhombic unitary cell with the dimensions $a = 1.07$ nm, $b = 0.595$ nm, and $c = 2.78$ nm.⁴⁹ De Santis and Kovacs have reported that the crystalline structure of poly(L-lactide) consists of left-handed helical chains.⁵⁰ The absence of peak shifts suggests that molecular distances in the crystalline structures are not affected and the two materials do not cocrystallize.

Scanning electron microscopy

The phase morphology of the PPD/PLLA system is shown in Figure 5. The SEM micrographs of surface revealed that the PLLA morphology is distinct from the PPD morphology. PPD presented an irregular surface, formed by sharp spheres, while PLLA has a rough surface less irregular. The SEM micrographs show that blends 40/60, 50/50, and 60/40 presented a nitid phase-separated morphology. On the other hand, the macroseparation is not visible for blends 20/80 and 80/20. The morphology observed for blends PPD/PLLA 20/80 and 80/20 systems showed more similarity with the pure component of respectively PLLA and PPD, probably due to the low concentration of the second component. However, a detailed analysis indicated that these blends also presented phase-separated morphology. Comparing blend PPD/PLLA 20/80 with the pure PLLA, small holes are detected, showing that the PLLA surface presents alterations with addition of only 20% of PPD in the blend. Blend 80/20 shows some smooth regions between PPD spheres, which can be attributed to PLLA. In the fracture surfaces, it is more clear that blends 20/80 and 80/20 also presents phase separation (Fig. 6). Iannace et al. also observed phase separation for all compositions and more similarity of blends PHB-HV/PLLA 20/80 and 80/20 with the pure polymer.¹⁷

Polarizing light microscopy

Figure 7 shows some typical micrographs of spherulites with a Maltese cross of PLLA and PPD for several blends. All the pictures show a space-filling crystallization. For pure PLLA crystallized at 130°C, we can see crystalline arrangements that grow until the crystallization process is limited by the increase of the spherulites in the neighborhood. The spherulites formation for pure PLLA is similar to those observed by Tsuji and Ikada for PLLA crystallized at 120, 140, and 160°C.²⁹ For pure PPD, crystallized at 65°C, regular concentric rings are observed which are not present in those of pure PLLA. The polarizing microscope observations revealed that PLLA could crystallize from the melt in the presence of PPD for all blend compositions. For blend PPD/PLLA 20/80, the spherulites coming from the crystallization of PPD are not observed, due probably to its low amount. For this blend, the biggest spherulites of PLLA grew at $T_c = 130^\circ\text{C}$, and the smaller grew during cooling to 65°C, because the sample was not kept at $T_c = 130^\circ\text{C}$ until it was completely crystallized and to fill all the space with the biggest spherulites. For temperatures lower than 130°C, the growth rate is higher and more nuclei are formed;

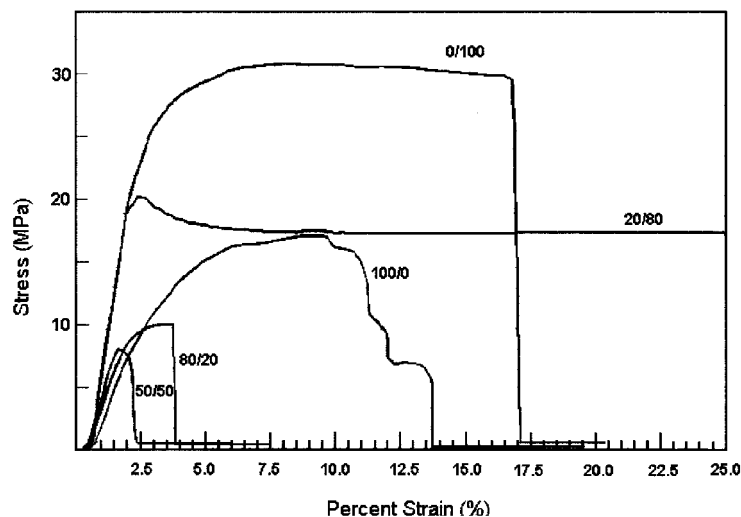


Figure 8 Stress-strain curves for PPD/PLLA blends.

consequently, a smaller but an increasing amount of spherulites are formed. Starting from the composition PPD/PLLA 40/60, it is possible to observe the presence of spherulites coming from both polymers. Although the content of PPD with reference to PLLA is high (40%), the PLLA spherulites are much more evident than PPD spherulites. For blend 50/50, macroseparation is observed, with well-defined domains of PLLA and PPD. With the increasing of PPD content in the blend, the macroseparation is not visible and for the blend 80/20, domains with PPD spherulites are seen that grew isolated from PLLA domains.

Mechanical properties

The mechanical behavior of the pure PLLA showed characteristics typical of glassy polymers with Young's modulus of 1402 ± 147 MPa, stress at break of 26 ± 3 MPa, tensile strength of 30 ± 2 MPa, elongation at break of $15 \pm 4.5\%$, and toughness of 3.9 ± 1.6 MPa. Figure 8 shows stress-strain curves for PPD/PLLA casting blends 0/100, 20/80, 50/50, 80/20, and 100/0, and Figure 9 shows the tensile properties of the blends. The mechanical behavior of PLLA is in agreement with the values reported by Jin,⁵¹ which obtained Young's modulus of 1582.5 MPa, stress at break of 18.1 MPa, and elongation at break of 10.2%. On the contrary, pure PPD exhibited lower Young's modulus than PLLA (584 ± 45 MPa), lower stress at break than PLLA ($11 \pm 4.4\%$), medium tensile strength (16.7 ± 1.5 MPa), almost the same elongation at break as pure PLLA ($14 \pm 4\%$), and lower toughness than PLLA (1.7 ± 0.6 MPa). The low value of Young's modulus gives high flexibility to PPD, due the presence of an ether bond

and an additional $-\text{CH}_2-$ in its backbone structure with reference to PLLA.¹² Figure 9 shows increased mechanical properties for blend 20/80. Adding only 20% of PPD to the PLLA phase, the system presents higher values of Young's modulus, elongation at break, and toughness than pure PLLA and PPD, while stress at break and tensile strength is lower than pure PLLA. These blends are more flexible, and tough material and neck formation during elongation is also observed, due to PPD, which may act as a plasticizer. An increase in elongation at break and neck formation was also observed for the PLLA/PEO blends containing more than 10 wt % of PEO.¹⁹ Overall mechanical properties of blends 50/50 and 80/20 were not improved. These blends presented Young's modulus higher than pure PPD, but lower values of stress at break, elongation at break, tensile strength, and toughness. For blend 50/50, this behavior might be connected with the nitid phase-separated morphology observed by SEM and PLM, resulting loss in the mechanical properties.

CONCLUSIONS

Two glass transition temperatures nearly constant and equal to the values of the homopolymers, and constant values of T_m were observed for all blend compositions, indicating that both polymers are immiscible. The PLM and SEM observations validated these results, and moreover, showed the different morphology obtained by changing the composition of the blend. The macroseparation was confirmed by SEM. However, for blends 20/80 and 80/20, the macroseparation was not so evident, probably due to the low amount of one component in the other. It was found by PLM that PPD is able to crystallize

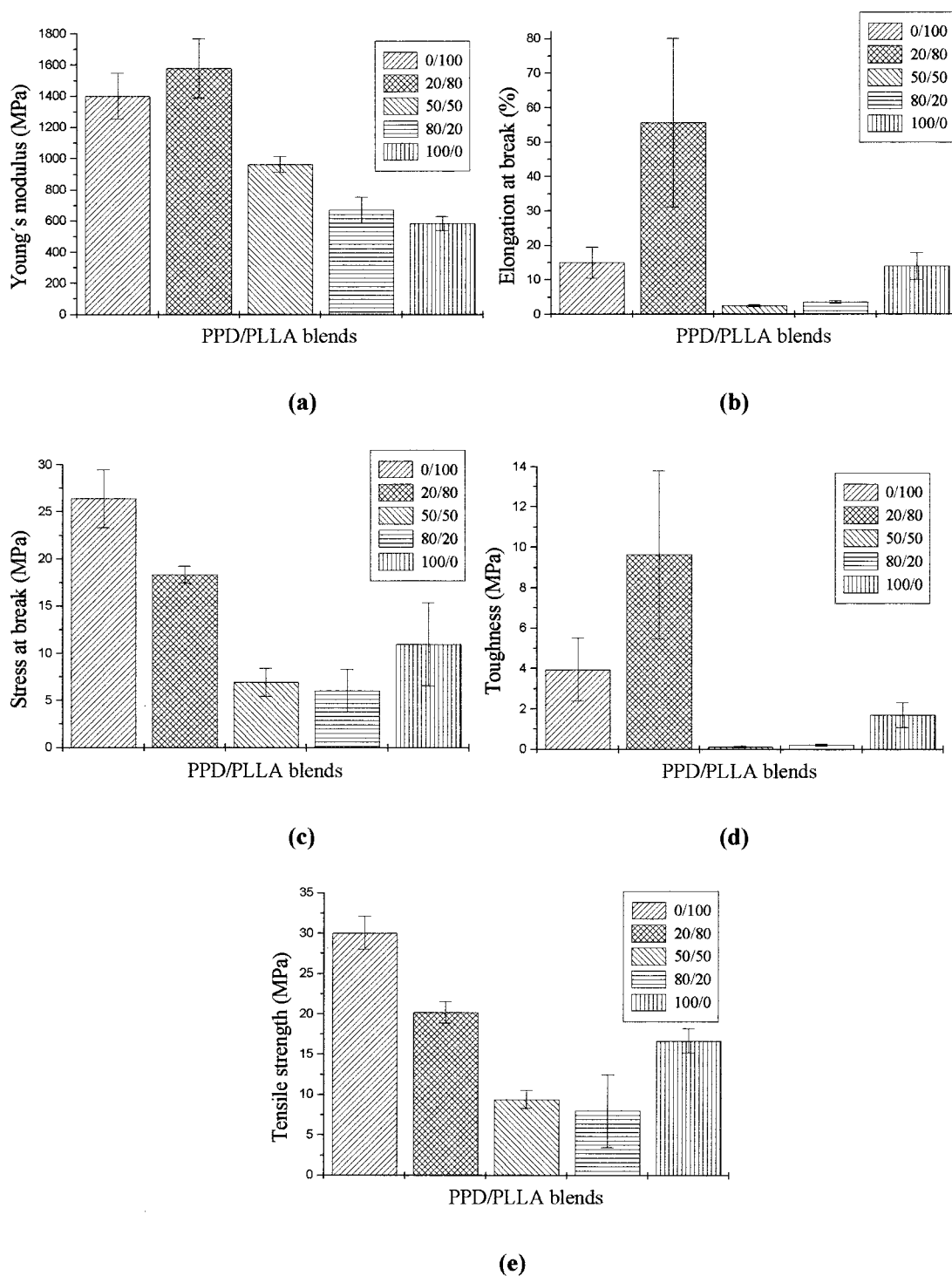


Figure 9 Tensile properties of PPD/PLLA blends. (a) Young's modulus, (b) elongation at break, (c) stress at break, (d) toughness, and (e) tensile strength.

according to a spherulitic morphology when its content is above 40%. Under this content, the crystallization of PPD is barely observed. Blend 20/80 is more flexible, and tough material and neck formation during elongation is also observed, due proba-

bly to PPD, which may act as a plasticizer. Studies about *in vitro* degradation of these blends are in progress in order to investigate the effect of the degradation of a single constituent on the properties of the multicomponent system.

References

1. Eguiburu, J. L.; Iruin, J. J.; Fernandez-Berridi, M. J.; San Román, J. *Polymer* 1998, 39, 6891.
2. Beiser, I. H.; Kanat, I. O. *J Am Podiat Med Assoc* 1990, 80, 72.
3. Hollinger, J.O.; Battistone, G. C. *Clin Orthopaed Related Res* 1986, 207, 291.
4. Vert, M.; Li, S. M.; Spenlehauer, G.; Guerin, P. *J Mater Sci: Mater Med* 1992, 3, 432.
5. Tsuji, H.; Hyon, S. H.; Ikada, Y. *Macromolecules* 1991, 24, 5657.
6. Tsuji, H.; Ikada, Y. *J Appl Polym Sci* 1997, 63, 855.
7. Zhang, L.; Goh, S. H.; Lee, S. Y. *Polymer* 1998, 39, 4841.
8. Nijenhuis, A. J.; Grijpma, D. W.; Pennings, A. J. *Polym Bull* 1991, 26, 71.
9. Doddi, N.; Versfelt, C. C.; Wasserman, D. U.S. Pat. no. 4,052,988, 1977.
10. Shalaby, S. W. *Biomedical Polymers: Designed-to-Degrade Systems*; Allen, A. L., et al., Eds. Hanser Publishers, 1994.
11. Chusak, R. B.; Dibbell, D. G. *Plastic Reconstructive Surg* 1983, 217.
12. Ray, J. A.; Doddi, N.; Regula, D.; Williams, J. A.; Melveger, A. *Surg Gynecol Obstet* 1981, 153, 497.
13. Lin, H. L.; Chu, C. C.; Grubb, D. J. *Biomed Mater Res* 1993, 27, 153.
14. Ibarra, C.; Jannetta, C.; Vacanti, C. A.; Cao, Y.; Kim, T. H.; Upton, J.; Vacanti, J. P. *Transplant Proc* 1997, 29, 986.
15. Pearce, R.; Marchessault, R. H. *Polymer* 1994, 35, 3990.
16. Vázquez-Torres, H.; Cruz-Ramos, C. A. *J Appl Polym Sci* 1994, 54, 1141.
17. Iannace, S.; Ambrosio, L.; Huang, S. J.; Nicolais, L. *J Appl Polym Sci* 1994, 54, 1525.
18. Penning, J. P.; St. John Manley, R. *Macromolecules* 1996, 29, 77.
19. Nijenhuis, A. J.; Colstee, E.; Grijpma, D. W.; Pennings, A. J. *Polymer* 1996, 37, 5849.
20. Ikada, Y.; Jamshidi, K.; Tsuji, H.; Hyon, S. H. *Macromolecules* 1987, 20, 904.
21. Tsuji, H.; Horii, F.; Hyon, S. H.; Ikada, Y. *Macromolecules* 1991, 24, 2719.
22. Tsuji, H. S.; Hyon, S. H.; Ikada, Y. *Macromolecules* 1991, 24, 5651.
23. Tsuji, H.; Hyon, S. H.; Ikada, Y. *Macromolecules* 1992, 25, 2940.
24. Tsuji, H.; Horii, F.; Naragawa, M.; Ikada, Y.; Odani, H.; Kitamaru, R. *Macromolecules* 1992, 25, 4114.
25. Tsuji, H.; Ikada, Y. *Macromolecules* 1993, 26, 6918.
26. Tsuji, H.; Ikada, Y.; Hyon, S. H.; Kimura, Y.; Kitao, T. *J Appl Polym Sci* 1994, 51, 337.
27. Tsuji, H.; Ikada, Y. *Polymer* 1999, 40, 6699.
28. Tsuji, H.; Ikada, Y. *Macromolecules* 1992, 25, 5719.
29. Tsuji, H.; Ikada, Y. *J Appl Polym Sci* 1995, 58, 1793.
30. Tsuji, H.; Ikada, Y. *Polymer* 1996, 37, 595.
31. Cha, Y.; Pitt, C. G. *Biomaterials* 1990, 11, 108.
32. Dijkstra, P. J.; Bulte, A.; Feijen, P. J. *Proceedings of the 17th Annual Meeting of the Society for Biomaterials, Scottsdale, AZ, Society for Biomaterials, Algonquin, IL, May 1-5, 1991*, 184.
33. Blümm, E.; Owen, A. J. *Polymer* 1995, 36, 4077.
34. Ferreira, B. M. P.; Zavaglia, C. A. C.; Duek, E. A. R. *Mater Res* 2001, 4, 34.
35. Dave, P. B.; Parikh, M.; Reeve, M.; Gross, R. A.; McCarthy, S. P. *Polym Mater Sci Eng* 1990, 63, 726.
36. Dave, P. B.; Ashar, N. J.; Gross, R. A.; McCarthy, S. P. *Polym Prepr* 1990, 31, 442.
37. Zhang, L.; Xiong, C.; Deng, X. *J Appl Polym Sci* 1995, 56, 103.
38. Tsuji, H.; Ikada, Y. *J Appl Polym Sci* 1996, 60, 2367.
39. Domb, A. J. *J Polym Sci, Part A: Polym Chem* 1993, 31, 1973.
40. Zhang, L.; Xiong, C.; Deng, X. *Polymer* 1996, 37, 235.
41. Organ, S. J. *Polymer* 1994, 35, 86.
42. Gassner, F.; Owen, A. J. *Polymer* 1994, 35, 2233.
43. Yasin, M.; Tighe, B. *J Plast Rubber Compos Process Appl* 1993, 19, 15.
44. Kumagai, Y.; Doi, Y. *Polym Degrad Stab* 1992, 36, 241.
45. Luciano, R. M. Master's thesis, Mechanical Engineering Faculty, State University of Campinas, São Paulo, 1995.
46. Reading, M.; Luget, A.; Wilson, R. *Thermochim Acta* 1994, 238, 295.
47. Fisher, E. W.; Sterzel, H. J.; Wegner, G. *Kolloid-ZZ Polimere* 1973, 251, 980.
48. Pezzin, A. P. T.; Alberda van Ekenstein, G. O. R.; Duek, E. A. R. *Polymer* 2001, 42, 8303.
49. Okihara, T.; Tsuji, M.; Kawaguchi, A.; Katayama, K.; Tsuji, H.; Hyon, S. H.; Ikada, Y. *J Macromol Sci, Phys* 1991, 25, 4114.
50. De Santis, P.; Kovacs, A. J. *Biopolymers* 1968, 6, 299.
51. Jin, H. J.; Chin, I. J.; Kim, M. N.; Kim, S. H.; Yoon, J. S. *Eur Polym J* 2000, 36, 165.